



Analysis of zero liquid disposal plant using electro dialysis integrated with electrolyzer for hydrogen fuel production

Emad Ali*, Abdelbasset Bessadok-Jemai

Chemical Engineering Department, King Saud University, Riyadh, Saudi Arabia, 11421, emails: amkamal@ksu.edu.sa (E. Ali), bessadok@ksu.edu.sa (A. Bessadok-Jemai)

Received 23 March 2022; Accepted 11 August 2022

ABSTRACT

This work proposes a plant for zero liquid discharge (ZLD) of a desalination plant waste. The plant uses an electro dialysis unit for salt concentration. In addition, the plant is augmented with an electrolyzer and fuel cell for hydrogen energy production. Several configurations were tested and compared to treat 100 m³/d of seawater fed to the desalination plant. The core operating condition of the ZLD plant is to concentrate 7.3% brine solution up to 12.5%. It is found that the best ZLD configuration can achieve 95% of overall water recovery, 6% liquid waste discharge, and 3,142 kg/d of solid salt production as added value. However, this performance requires a specific energy demand of 900 kWh/m³. This considerable energy demand is attributed to the electrolyzer which consumes 98% of the total energy requirement. It is found that the energy produced by the fuel cell can cover 80% of the energy required by the electrolyzer. It is also found that attaining full zero waste discharge via recycling the waste liquid back to the process limits the operational range of the process components and may deteriorate the process operation.

Keywords: Water desalination; Brine disposal; Zero liquid discharge; Electrolyzer; Fuel cell

1. Introduction

No doubt that saline water desalination became a major source of drinkable water around the globe to overcome freshwater shortages [1]. This issue is intensifying as population and industrialization grow rapidly [2] causing massive expansion in the installed and projected desalination capacity [3,4]. Regardless of their respective variation, desalination technologies suffer from two main issues; high energy consumption [2,5] and waste disposal [6]. The first issue derived ample research activities to develop energy-efficient and hence cost-effective desalination technologies [3]. On the other hand, desalination waste disposal causes a detrimental effect on the environment because the current common practice of waste disposal is discarding into ocean and surface water [7]. Conventional desalination plants have a limited recovery ratio. For example,

membrane desalination technology comprises 65%~68% of total desalination plants [7,8]. However, reverse osmosis (RO)-based desalination has a water recovery ratio of 45%, which can reach 75%~85% for brackish water. This implies that 55%~15% of the saline water must be disposed to the environment as reject concentrate [9]. According to Panagopoulos et al. [10] the discard of RO brine comprises 33% of the total operational cost contingent on the reject capacity, concentration, and disposal option. Other desalination technologies have even larger reject disposal. For example, the recovery of multistage flash desalination is 25%~50% [11] and the recovery of the multi-effect evaporator is 25%~35% [12]. Moreover, saline wastewater is generated from several industries other than desalination [6,13]. Zhang et al. [6] discussed the conventional waste disposal methods. They reported that in the USA 70% of the desalination plants use surface/sewer discharge, 17%

* Corresponding author.

use deep-well injection, and 7% use land application for brine disposal. Other reported options are evaporation ponds, wind-based evaporation, and mist spray. Ahmed et al. [14] pointed out that surface/sewer discharge of brine influences groundwater characteristics, crops, and civic sewage management system. Although deep-well injection and evaporation are less harmful ecologically, they are economically relatively more intensive.

An alternative sustainable solution to waste disposal is the so call zero liquid discharge (ZLD) system. ZLD systems are designed to generate additional potable water and value-added salt with no liquid waste discard [7]. This process received considerable attention in the past ten years, especially in the USA, China, and India [13,15]. However, the standard thermal ZLD systems suffer from high cost [15]. This situation pushed researchers to pursue alternative technologies, novel strategies, or retrofitting that are economically feasible. The core of ZLD processes is the concentrator which concentrates the brine solution to the edge of the saturation limit before being sent to crystallizer or evaporation ponds to produce valuable salt crystals. Usually, evaporators such as mechanical vapor compression (MVC) are utilized for the concentration step. However, the MVC unit is energy-intensive. Thiel et al. [16] reported energy consumption in the range of 23–42 kWh/m³ of distillate for a single-stage MVC. McGinnis et al. [17] has recorded energy demand values from 28 to 39 kWh/m³ of feed for an MVC in a pilot plant used to treat wastewater with an inlet concentration between 45,000 and 80,000 ppm. Others have studied the use of membrane distillation (MD) as a salt concentrator. For example, Lu et al. [7] studied a pilot-scale ZLD system of 72 kg/d capacity comprises of freeze desalination coupled with MD-crystallization units. The plant receives 50% of its heating energy from solar panels and a 100% of its cooling from liquid natural gas. Although zero liquid discharge is obtained but at dramatic energy demand. Schwantes et al. [15] also investigated the economics of using air gap MD in a ZLD process. They reported a 40% improvement in the energy consumption compared to MVC for a plant capacity of 100 m³/d of saline feed. Zhang et al. [6] similarly studied the utilization of direct contact membrane distillation (DCMD) to concentrate the brine produced from the brackish water RO plant. They concluded that MD was able to improve the overall water recovery to almost 90%. However, proper pre-treatment of the RO concentrate is crucial to achieving the desired performance. Many other researchers have also investigated the use of MD in ZLD systems [18–20]. Nevertheless, MD is known for high specific energy demand around 39–60 kWh/m³ [13] and a low recovery ratio for a single pass in the range of 5%–7% [21]. Moreover, operating MD at very high salinity may expedite fouling [22]. Thereby, to achieve a high recovery ratio, multiple MD modules in series are required which will intensify the total required energy demand. Other treatment technologies were also studied. For example, Lawal et al. [23] investigated the use of humidification and dehumidification (HDH) to treat the MSF brine where 67% pure water was recovered. Similarly, Tahir and Al-Ghamdi [22] studied the integration of HDH with MED to minimize liquid discharge. Other researchers considered using

electrodialysis (ED), which is an electrically driven process, to concentrate waste brine. Loganathan et al. [24] used a pilot plant to prove the concept of integrating an electro-dialysis reversal and reverse RO to treat basal water to achieve near-zero liquid disposal. The hybrid ZLD system was found to recover 77% of the basal water and concentrate the brine up to 12.5%. Davis [25] proposed using electro-dialysis (ED) to dilute the brine of seawater RO (SWRO) plant with a portion of it recycled to the SWRO plant and the rest is treated to extract Mg(OH)₂. The ED concentrate, which can reach 23%, is further concentrated via evaporator and then sent to crystallizer for NaCl generation. However, the high capital cost and specific power consumption of the existing ZLD systems hinder their utilization in water and salt recovery from seawater and brackish water desalination [25]. Nevertheless, ED is widely used on a large scale to extract commercial salt from seawater. Moreover, it has energy reduction features and can be fine-tuned to produce a dilute stream equivalent to the seawater characteristics which makes its discharge harmless [25]. A review of different pre-treatment and brine concentration technologies for ZLD systems can be found by the study of Panagopoulos et al. [10].

In this work, the ZLD system is revisited using ED as a brine concentrator due to its appealing features. The system is augmented with electrolysis and fuel cell for electrical energy production as value-added items or to partially subsidize the energy demand of the ZLD system.

Several process scenarios will be considered consisting of retrofitting seawater brine waste management unit operations to an existing desalination plant. This study will focus on the synergetic integration of ED and electrolyzer (EZ). Different structures to optimize the process performance are also proposed. The reflection of the varied structures on the overall performance will be analyzed. Furthermore, the impact of the variation in the structures on the performance of the individual unit will be examined. This will help identify the benefits and/or limitations incurred by these modifications.

2. ZLD process description

The main objective of the ZLD process is to eliminate the liquid discharge of a typical desalination plant. The ZLD also produces commercial salt crystals and pure water as added value. In this study, we investigate producing renewable energy as another value-added product.

Fig. 1 depicts the proposed process for zero-waste production. Saline seawater of around 40,000 ppm is desalinated in a separate desalination unit. In this study, the MSF plant is considered for desalination with 40% recovery. The desalination waste, basically reject brine, is fed into the treatment process. First, the brine is treated using nanofiltration (NF) to remove most of the total dissolved solids (TDS) other than NaCl. Hence, NF works as a pre-concentrator where the large portion of NaCl is separated from the rest of TDS. Since NF is a pressure-driven process, the feed is pressurized to the desired pressure using a pump. The permeate effluent of the NF is fed to the concentrator, which is an electro-dialysis (ED) unit driven by electric power. The concentrated solution (as a

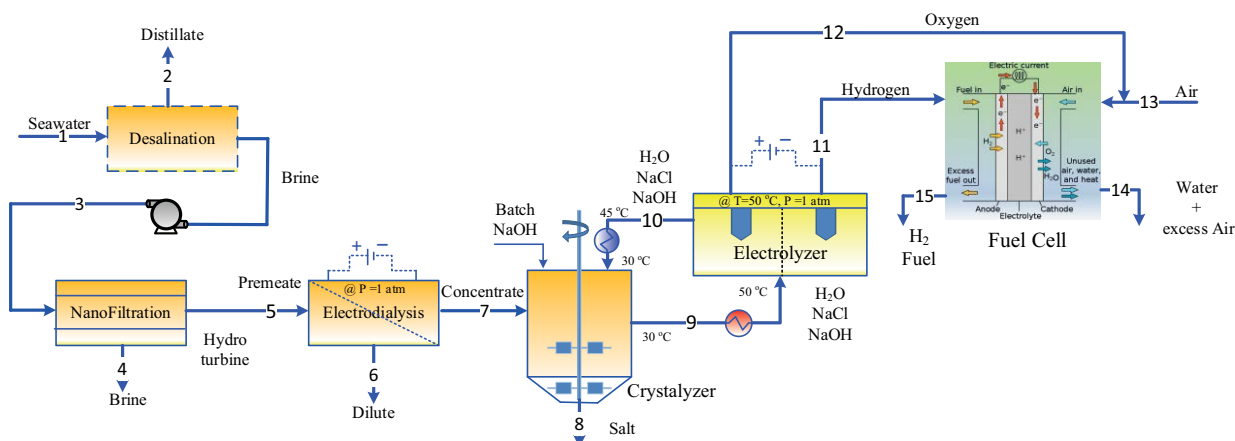


Fig. 1. Schematic of the (configuration S1).

case study around 125,000 ppm at nominal conditions) is then fed into the crystallizer where solid salt and highly pure water are produced. The highly pure water is used to generate hydrogen fuel via a series of electrolyzer (EZ) and fuel cell (FC). The produced pure water is regenerated again in the fuel cell. The EZ works at about 50 °C, therefore, the feed needs to be heated. Similarly, the effluent of the EZ unit must be cooled down to the operating temperature of the crystallizer. It is assumed here that heat integration is utilized such that the EZ influent gains 10 °C from the EZ effluent. Thereby, the EZ influent will be further heated by 10 °C using an external energy source. Similarly, the EZ effluent will be cooled by another 5 °C from any auxiliary cold stream in the plant.

Note that effluent streams 4 and 6 are discharged as waste because they are not suitable for drinkable water, that is, their salinity is higher than 500 ppm, which is the standard set by the World Health Organization (WHO) [26,27]. Thereby, zero liquid discharge is not fully attained. Usually, other ZLD systems revert to recycling the waste stream back to the system. Although this practice may be harmful to the process, that is, accelerates fouling in membrane-based units, it will be considered here for analysis. For this reason, three modification scenarios of S1 are considered as shown in Fig. 2. Note, that stream 4 is small in magnitude due to NF high recovery considered here and it is highly saline and populated with undesired TDS. Hence, it is not recommended to recycle back to the NF unit. On the other hand, stream 6 is diluted and contains a large amount of water depending on the operating condition of the ED. Therefore, stream 6 can be recycled solely to join the NF feed and denoted as scenario S1a. Alternatively, stream 6 can be recycled to join the ED feed which is denoted as scenario S1b. A third option is to mix stream 6 with 4 and recycle to join the NF feed. Since stream 6 is diluted and has a relatively larger flow rate than stream 4, the latter will be diluted enough to be fed to the NF. Note it is important that the recycle stream be less concentrated than the main feed of the NF to reduce the required transmembrane pressure. The objective of recycling is to eliminate waste rejection, that is, achieving the zero liquid discharge requirement. However, depending on the

solution composition and operating conditions, recycling may deteriorate the performance of the NF and/or ED. It should be noted that for S1a, the recycle stream needs to be pressurized to meet the NF pressure requirement.

Another modification of the basic structure (S1) is to add an RO to treat stream 6 as demonstrated in Fig. 3. Since stream 6 is diluted, RO is a suitable system to treat it, that is, to extract additional pure water and reduce the reject concentrate. But additional power is needed to pressurize the RO feed to the required pressure to overcome the osmotic pressure. Of course, the RO effluent, streams 16 and 17 can be de-pressurized to recover their energy. The objective of the RO system is to reduce the waste discharge as stream 16 will be much less than stream 6. Moreover, the RO will extract additional pure water to promote the energy production of the FC and at the same time promote the overall water recovery. Hence, the incorporation of an RO will have some added value at low additional energy requirements because the RO feed is diluted and a portion of the pressurizing energy will be recovered. In fact, it is reported that using RO to treat the ED not only increases the recovery but also improves the RO performance [24]. In this case, the ED acts as a pre-treatment for the RO feed causing a reduction of the osmotic pressure of the RO feed. Nevertheless, the heating requirement in the heat exchanger to increase the temperature of the EZ feed will be increased. Moreover, the waste discharge does not approach zero like in the S1c structure. For this purpose, variants of S2 can be considered as shown in Fig. 4. To reduce the liquid discharge, stream 16 can be either recycled to the NF feed comprising structure S2a or recycled to the ED feed comprising structure S2b. For S2a, a booster pump is needed provided that the NF operates at a higher pressure than the RO. For S2b, the pressure of stream 16 should be recovered before injection into the ED.

A third structure denoted S3 is proposed as illustrated in Fig. 5. In this case, RO is utilized as a concentrator instead of the ED. Generally, RO is not recommended for this purpose [15]. Nevertheless, it was utilized for investigation purposes bearing in mind that the RO feed salinity is around 50,000 ppm in this study. Alternatively improved versions of RO such as high-pressure RO (HPRO) or osmotically assisted reverse osmosis (OARO) can be utilized.

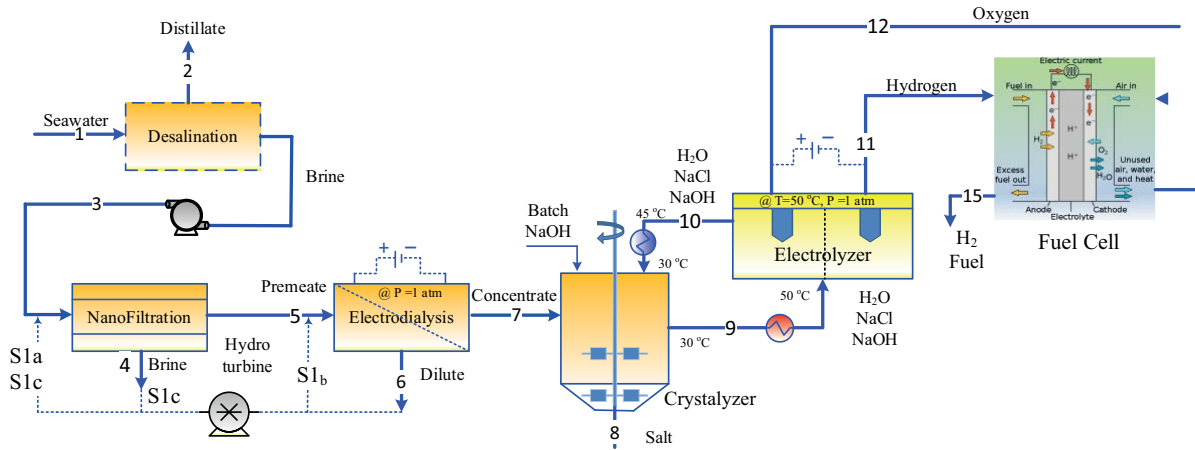


Fig. 2. Modified S1 structures.

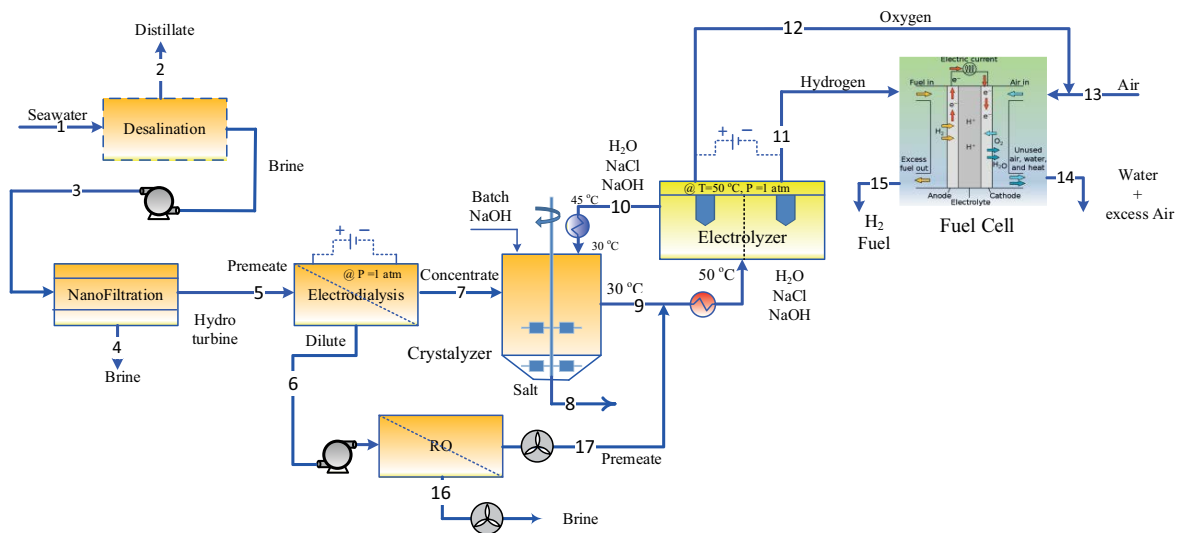


Fig. 3. Schematic of S2 configuration.

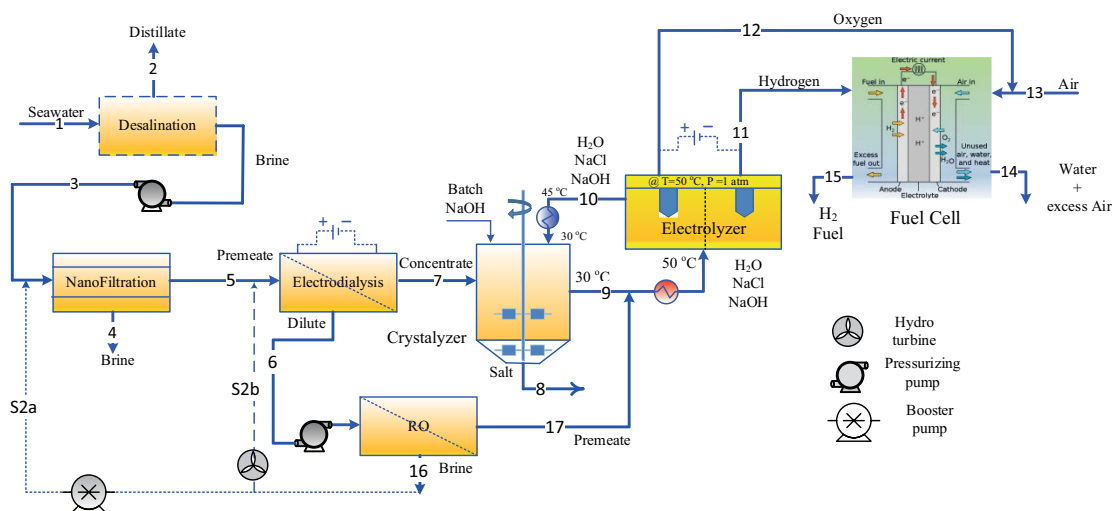


Fig. 4. Variants of structure S2.

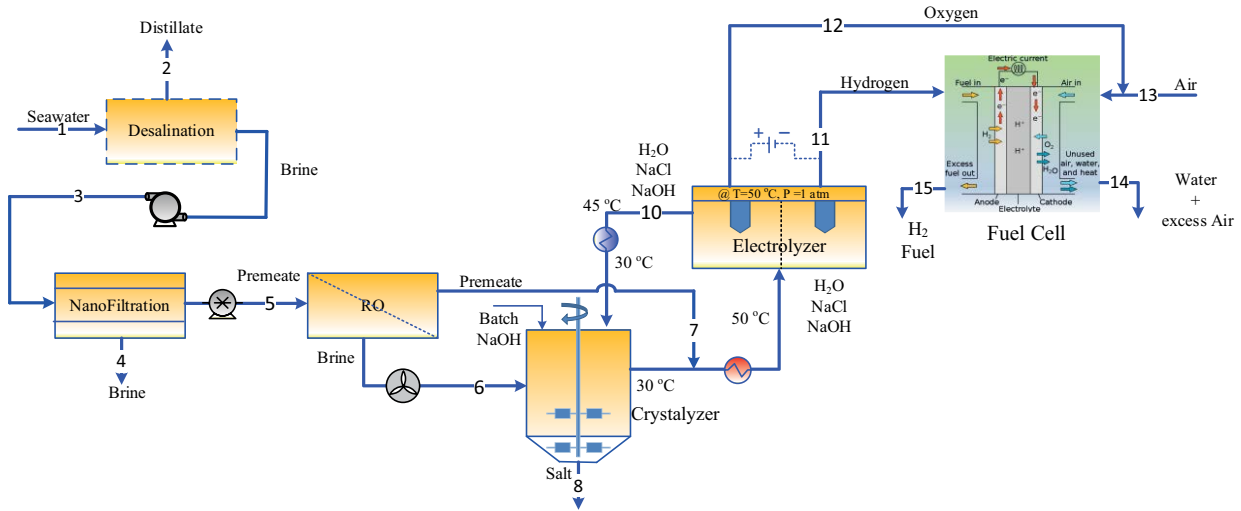


Fig. 5. Schematic of structure S3.

HPRO and OARO can treat much higher feed salinity than standard RO [13]. In this case, the RO is operated at the highest possible feed pressure of 85 bar [28] to achieve the highest possible concentration in the brine. This will sacrifice the recovery ratio of the RO. Hence, the RO model is solved such that to find the highest possible recovery ratio that does not necessitate feed pressure higher than 85 bar. Like S1a, S1b, S2a, and S2b, this structure can reduce the waste liquid discharge to stream 4 exclusively. A booster pump is required to increase stream 5 pressure to the required RO pressure. Of course, the energy associated with the RO effluent can be recovered via the hydro-turbines. It is also expected that the energy requirement of the EZ feed increases for two reasons. First, the mass flow rate of the EZ feed will be higher. Secondly, the heat recovered from the cooler by heat integration as mentioned earlier cannot provide a 10°C increment in the EZ feed because of the different relative mass rates.

The nominal operating condition of the proposed system is listed in Table 1. The desalination plant is taken as MSF such that ultra-pure water is produced and all TDS are transferred to the brine stream, that is, stream 3. The seawater TDS is listed in Table 2. These parameters are used to solve the plant mass balance and energy requirements. For analysis and comparison purposes, specific key performance parameters are used as described in the following.

Overall water recovery ratio:

$$RR = \frac{m_2 + m_{14,w}}{m_1} \times 100 \quad (1)$$

Solid salt production, kg/d:

$$S = m_{8,s} \quad (2)$$

Waste liquid rejection ratio:

$$Rej = \frac{m_4 + m_6 + m_{16}}{m_1} \times 100 \quad (3)$$

Total required power, kW:

$$TRP = P_{w,NF} + P_{w,RO} + P_{w,ED} + P_{w,EZ} + P_{HE} + P_{w,boost} \quad (4)$$

Total generated power, kW:

$$TGP = P_{w,FC} + \sum P_{w,R} \quad (5)$$

Gross power requirements, kW:

$$GP_w = TRP - TGP \quad (6)$$

Specific gross power requirement, kWh/m³:

$$GP_{ws} = \frac{GP_w \times 24}{(m_2 + m_{14,w}) / \rho} \quad (7)$$

The pumping power and recovered power are calculated as follows:

$$P_{wp} = \frac{Q\Delta P}{\eta_p} \quad (8)$$

$$P_{wR} = Q\Delta P / \eta_R \quad (9)$$

where Q is the volumetric flow rate in m³/s, ΔP is the pressure difference in Pa and η is the unit efficiency. The generated power is in W.

It should be noted, that the terms involved in the liquid rejection rate [Eq. (3)] depend on the structure used. For example, some structures exclude streams 6 or 16. Similarly, the terms involved in computing the total required power [Eq. (4)] depend on the selected configuration. For example, some structures exclude the RO power. Generally, the specific energy is computed as the ratio of the energy demand to the seawater feed rate. This makes the specific energy proportional to the energy demand because the seawater feed is constant. Since the ZLD process produces

Table 1
Nominal operating condition of the proposed process

m_f	Seawater feed rate, m ³ /d	100
T	Seawater feed temperature, °C	25
RR	Desalination recovery ratio	0.4
RR _{NF}	NF recovery ratio	0.9
RR _{RO}	RO recovery ratio	0.7
Rjs	NaCl rejection in NF	0.2 [28]
Rji	TDS rejection in NF	0.98 [28]
DR	NaCl depletion rate in ED	0.85 [34]
Csc	NaCl fraction in ED concentrated product	0.125 [39]
Xs	Fraction of NaCl in solid product	0.95
Ws	Solubility of NaOH in water, kg NaOH/kg H ₂ O	0.3 [39]
Ns	Solubility of NaCl in water, kg NaCl/kg water	0.15 [39]
O ₂ excess	Oxygen excess in FC	0.25
J_{FC}	FC current density, kAmp/m ²	4 [39,44]
V_{FC}	FC cell voltage, volt	0.68 [44]
A _{eff} _{FC}	FC cell effective area, m ²	1 [44]
η_{FC}	FC efficiency	0.55 [44]
J_{EZ}	EZ current density, kAmp/m ²	4.67 [41]
V_{EZ}	EZ cell voltage, volt	2.75 [41]
A _{eff} _{EZ}	Effective area, m ²	1 [41]
η_{EZ}	EZ efficiency	0.85 [41]
η_{ED}	ED electric efficiency	0.85 [41]
id	ED current density, kAmps/m ²	0.4 [34]
a _{eff}	ED membrane area efficiency	0.9 [34]
V_{ED}	ED cell voltage, Volt	0.8 [34]
η_{HT}	Hydro-turbine efficiency	0.7

Table 2
Seawater composition

Ion	ppm
Cl ⁻	24,090
Na ⁺	13,400
SO ₄ ⁻	3,384
Mg ⁺⁺	1,618
Ca ⁺⁺	508
K ⁺	483
HCO ₃ ⁻	130
Br ⁻	83
Si ⁺	0.09

pure water beyond the desalination process, it is of interest to define the specific energy as a ratio of the energy demand to the produced pure water.

2.1. RO unit

RO is well known for being energy-efficient with the specific energy demand of 2–4.5 kWh/m³ of feed [29]. Due to limitations imposed by osmotic pressure, RO is typically used for salinity less than 70,000 ppm [30]. RO is used here

to further recover clean water from the ED reject. It is also tested for salt concentration for demonstration purposes. The model for RO has been well established for decades. Since our objective here is not to develop a new model, we adopt the one proposed by Kumarasamy et al. [27].

The permeate production rate (Q_p) is defined as:

$$Q_p = A \times S_A (P_f - \pi_{ave}PF + \pi_p) \tag{10}$$

where A is the permeability of water (0.0148 m/d/bar), S_A is the surface area taken as 400 m² here, and P_f is the feed pressure to be calculated to achieve the desired recovery ratio. The polarization factor (PF), the average osmotic pressure (π_{ave}), and the osmotic pressure of the permeate (π_p) are calculated as follows:

$$\pi_p = 7.857 \times 10^{-4} \times C_p \tag{11}$$

$$\pi_{ave} = 7.857 \times 10^{-4} \times \frac{C_f + C_b}{2} \tag{12}$$

$$PF = \exp\left(\frac{KQ_p}{Q_f}\right) \tag{13}$$

where $K = 0.0491$, C_b is the brine concentration to be computed from salt balance, C_f is the feed concentration, and Q_f is

the feed flow rate. The permeate concentration, C_p is computed as follows:

$$C_p = B \times S \times C_{ave} \times \frac{PF}{Q_p} \quad (14)$$

where the salt permeability $B = 0.0027$ m/d. The power requirement of RO ($P_{w,RO}$) can be calculated using Eq. (8).

2.2. NF unit

The nanofiltration is the first unit in the proposed ZLD process. NF act as a pre-concentrator where it recovers NaCl from the desalination concentrate and rejects most of the TDS. NF is a membrane unit powered by hydraulic pressure with performance lies between ultrafiltration and reverse osmosis. NF operates at a lower operating pressure and provides higher recovery than RO and greater rejection than ultrafiltration [31]. NF is known for treating scaling ions, organic matter, and silica [13]. As mentioned earlier, it is not the focus here to develop a rigorous model for the NF unit. Hence, we adopt the NF model given by Ghorbani et al. [31] and Roy et al. [32].

Given the recovery ratio (R_{NF}), the permeate flow rate is given by:

$$Q = R_{NF} Q_f = J_w S_A \quad (15)$$

where J_w is the solvent flux across the membrane and S_A is the surface area taken as 200 m² in this study. The solvent mass flux is defined as follows:

$$J_w = (P_f - P_p - \pi) \left(\frac{r_{pore}^2}{\mu \left(\frac{\Delta x}{A_k} \right)} \right) \quad (16)$$

where P_p is the permeate pressure, p is the transmembrane osmotic pressure given by Eq. (11), and m is the solvent viscosity. r_{pore} is the pore radius equal to 0.43 nm, and $(\Delta x/A_k)$ is the active layer thickness to porosity ratio and equal to 1 μ m. We consider the membrane has selective rejection towards dissolved salts with a 98% rejection rate and 20% for NaCl [28]. Hence the distribution of the TDS in the NF brine is as follows:

$$Q_{b,s} = R_{j,s} Q_{f,s} \quad (17)$$

$$Q_{b,NaCl} = R_{j,NaCl} Q_{f,NaCl} \quad (18)$$

where $R_{j,s}$ is the rejection ratio for dissolved salt and $R_{j,NaCl}$ is the reject rate for sodium chloride. The power requirement of the NF ($P_{w,NF}$) can be calculated from Eq. 8.

2.3. ED unit

Electrodialysis (ED) is an electrochemically driven separation technique involving ions transfer across ion-selective membranes as means to concentrate salt solution or brackish waters [33–35]. A salt solution feed can thus be

subdivided into dilute and concentrated phases (Fig. 6). Depending on the objective of the ED separation, the product could be either the dilute or the concentrated phase. This means that the dilute phase is the product when the removal of ions is to be achieved to below a targeted concentration level (e.g., potable water). While the concentrate phase is the product if ions have to be accumulated to above a targeted level, (e.g., production of valuable ionic solutions) [34].

Fig. 6 illustrates the principle of conventional ED in the form of electro dialysis cell configuration constituted of a series of anion- and cation exchange membranes (AEMs and CEMs, respectively). These membranes are alternately placed in series between two electrodes (e.g., the anode (+) and the cathode (-)). The ion transport between membranes is insured by the application of an applied electrical potential (ion-exchange driving force). During operation, CEMs allow only the passage of cations (-) while the anions (+) are rejected. Oppositely, the AEMs allow only the passage of anions and reject the cations. In this way, charged anions and cations would be trapped between two adjacent CEM-AEM (concentrated phase), whereas the ion-depleted phase transits between each two adjacent AEM-CEM (dilute phase).

The electrodes are placed in a separated compartment through which an electrolytic solution is constantly passed to protect the electrodes from the feed solution. The electrolytic solution should be regenerated once in a while to compensate for contamination or leakage from the process stream to the electrodes compartment. A repeating unit composed of successive CEM-AEM is called cell pair (3 membranes and 2 spacings). An ED stack is equipment composed of a number of cell pairs capped with two electrodes at both ends. In industrial practices, a common stack typically contains up to 600 cell pairs in addition to the electrodes [34].

As depicted in Fig. 6, the mass transport through a cell pair occurs in two compartments, namely the dilute and the concentrate phases and each chamber is separated by the sequence of AEM and CEM. Transport occurs as a result of differences between the dilute and concentrate solution across the membranes (z-direction) and by convection of the solutions parallel to liquid flow (x-direction) in and out of the cells. It should be noted however that the diffusive salt flux in the x-direction is negligibly small compared to the convective flux in this direction [36].

The salt depletion rate is the ratio of the amount of salt transferred from the feed brine to the concentrated stream; it is defined as follows:

$$DR = 1 - \frac{m_s^d}{m_s^f} = \frac{m_s^c}{m_s^f} \quad (19)$$

The salt depletion rate can also be obtained based on the ionic rates $\dot{C} \left(\frac{k_{eq}}{s} \right)$ by:

$$DR = 1 - \frac{\dot{C}_s^d}{\dot{C}_s^f} = \frac{\text{ions}_s^c}{\text{ions}_s^f} \quad (20)$$

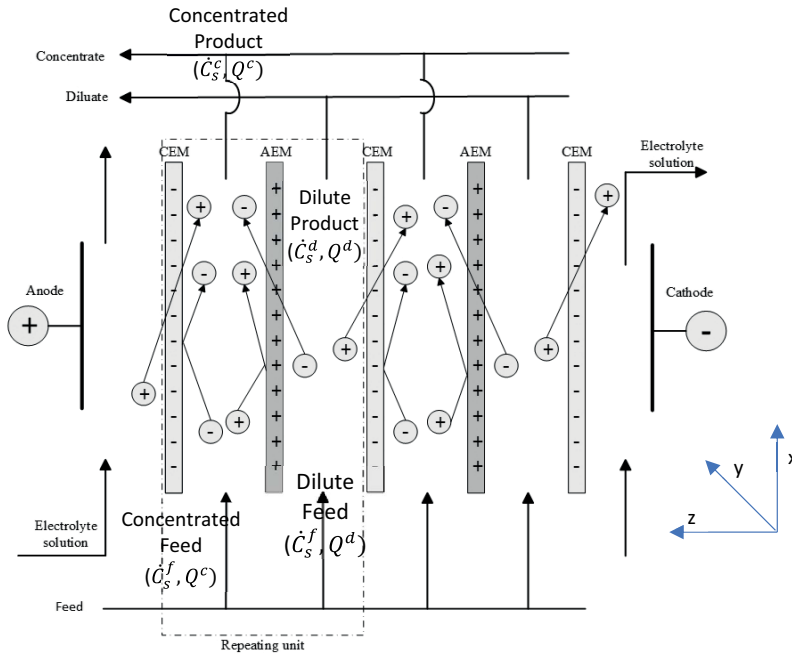


Fig. 6. Schematic illustration of the principle of desalination by ED in a stack with AEMs and CEMs in alternating series between two electrodes [34].

The ions transport through the membranes results from the application of an electrical potential difference (V); this mass transport is, in fact, proportional to the electrical current (I) passing through the cell pair. The ionic fluxes from dilute to concentrate solutions lead to differences in concentration between the feed and the exit through both channels.

A material balance of mass transport within an ED stack is given in the following design equation:

$$(\dot{C}_s^f - \dot{C}_s^d)Q_d = (\dot{C}_s^c - \dot{C}_s^f)Q_c = \frac{N \cdot \xi \cdot I}{DR \cdot z \cdot F} \quad (21)$$

The superscripts (d) and (c) refer to the dilute and concentrate cell inlets, the superscripts (d) and (c) refer to dilute and concentrate and the subscripts (s) and (c) refer to salt solution and cation. The current utilization, ξ , is a measure of the amount of total current through an ED stack that can be utilized for the removal of the ions from the feed. The current efficiency is always <1 because of inevitable energy losses and is commonly from 80% to 95% [34].

The required electrical power for the ED can be computed as follows:

$$P_{w,ED} = \eta_{el} \times I \times V \times N \quad (22)$$

2.4. Crystalliser unit

This unit is a crystallization/recycling tank (CR) placed between the ED and the electrolyzer (EZ) units as shown in Fig. 7. It serves as a mixer/settler recycling tank in which the concentrated brine (from the ED) is mixed with a start-up saturated solution (fixed initial quantity with

an added salt seed for nucleation) forming a mix to feed the EZ; Excess NaCl in the saturated mix continuously crystallizes to form salt crystals. The start-up solution should be saturated in NaCl (at the operating temperature of $\sim 30^\circ\text{C}$) and contains NaOH and H_2O at mass fractions ($\text{H}_2\text{O}:\text{NaOH}:\text{NaCl} = 1:0.3:0.15$)³⁸.

The main operating parameters of the CR step are the magma flowrate (brine + EZ recycle) \dot{v} (m^3/s), the crystal growth rate G (m/s), the residence time t_r (s), the mean crystal size L_m (m), the mixture volume V_{mix} (m^3), and the tank volume V_{tank} (m^3).

Typical residence times vary from 1 to 4 h, while the mean crystal sizes range from 0.2 to 1.2 mm [37]. A seed salt quantity ranging from 0.1% to 3% of the slurry mix is initially introduced (say 0.5% seed) to initiate nucleation and subsequently crystal growth in the mix [38].

The growth rate is defined by:

$$G = \frac{30.2}{k_R k_V \rho_c L_m^4} \quad (23)$$

where k_R and k_V are the rate constant and crystal shape factor [39,40] equal to $2.6 \cdot 10^{16}$ and 1.05, respectively; while ρ_c is the salt crystals density ($2,170 \text{ kg}/\text{m}^3$).

The crystallizer magma residence time may be estimated by the following:

$$t_r = \frac{L_m}{3.67G} \quad (24)$$

The mix volume is related to the residence time by the following equation:

$$V_{\text{mix}} = \dot{v} t_r \quad (25)$$

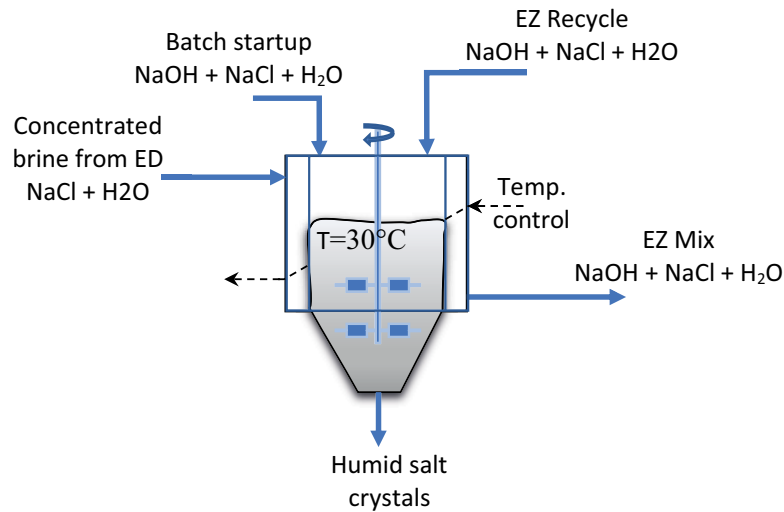


Fig. 7. Schematic illustration of the settling/crystallization tank.

The tank volume may be estimated by a choice of common tank diameter (e.g., 1–1.5 m) and an adequate H/D ratio (e.g., $(H/D)_{\text{ratio}} = 1.5\text{--}3$). Thus, the tank volume could be estimated by the following relation:

$$V_{\text{tank}} = \pi \cdot \frac{D^2}{4} \times \left(\frac{H}{D}\right)_{\text{ratio}} \times D \quad (26)$$

If a tank fill fraction (ff) is to be insured, then the tank volume maybe estimated by :

$$V_{\text{tank}} = \frac{V_{\text{mix}}}{\text{ff}} \quad (27)$$

Table 3 gives a rough estimate of the CR operating parameters; these data are obtained for a choice of tank diameter (e.g., $D = 1, 1.25$ and 1.5 m), a height-to-diameter ratio (e.g., $(H/D)_{\text{ratio}} = 3, 2.25$, and 1.5), and fill ratio $\text{ff} = 85\%$. Option 2 in Table 3 may be used as a design scenario. The required power for the CR (P_{HE}) is simply the sensible heat needed to heat the ED effluent.

2.5. Electrolyzer unit

Electrolytic induced reactions in a chlorine-free alkaline electrolyzer (EZ) simply reduce to water splitting electrolysis producing oxygen and hydrogen. Indeed, recent advances in seawater brine treatment suggest that the development of special metal-oxides coated electrodes favors oxygen evolution reaction (OER) while hindering chlorine formation at the anode [38,40]. Typical EZ practice data and the present design assumptions are given in Table 4.

From electrochemistry principles, the total charges \tilde{Q} (Coulombs) for 1 cell/d is defined by [41,42]:

$$\begin{aligned} \tilde{Q}_{\text{1cell}} &= \text{electric current (Amps)} \times \text{time (sec)} \\ &= I \times 24 \times 3,600 \text{ (in Amps-s/cell)} \\ &= 86,400 \times I \text{ (in Amps-s/cell)} \end{aligned} \quad (28)$$

The daily hydrogen molar production rate for 1 cell is

$$\begin{aligned} \dot{m}_{H_2}^{(\text{1cell})} &= \tilde{Q}_{\text{1cell}} (\text{Amps-s}) \times \frac{1(\text{mol} \cdot e^-)}{F(C)} \times \frac{1(\text{mol} \cdot H_2)}{2(\text{mol} \cdot e^-)} \\ &= \frac{86,400 \times I}{2 \times F} \left(\text{mol} \cdot \frac{H_2}{d} \text{ per cell} \right) \end{aligned} \quad (29)$$

For an ideal electrolyzer (100% efficiency), the number of cells will then be computed by:

$$N_{\text{cell,EZ}} = \frac{\dot{m}_{H_2}^{(\text{total})}}{\dot{m}_{H_2}^{(\text{1cell})}} (\text{cells}) \quad (30)$$

$$\tilde{Q}_{\text{total}} = N_{\text{cell,EZ}} \times \tilde{Q}_{\text{1cell}} = N_{\text{cell}} \times I \times 86,400 \text{ (in C/cell)} \quad (31)$$

The power requirement of the EZ can be computed as follows:

$$P_{w,EZ} = \frac{1}{\eta_{EZ}} \times N_{\text{cell,EZ}} \times I_{\text{cell,EZ}} \times V_{\text{cell,EZ}} \quad (32)$$

The EZ design data are found in Table 4.

2.6. Fuel cell unit

Nowadays, hydrogen is an energy sector that can be used to power nearly every end-use energy need on small, medium, and large scales. This can be achieved by the use of what is known as fuel cells; these are key energy conversion devices that can effectively make use of the power of hydrogen to produce electrical energy to power various systems.

Fig. 8 is a schematic of a fuel cell, a sandwich-type arrangement in which an electrolyte is placed between two electrodes. In addition, a bipolar plate on the two end sides serves to distribute gases and as current collectors. Most widely used, a polymer electrolyte membrane (PEM) fuel cell causes the entering gas (H_2) at its anode, to dissociate

Table 3
Data for estimating CR operating parameters

Parameter	Option 1	Option 2	Option 3
Tank diameter, D (m)	1	1.25	1.5
$(H/D)_{ratio}$ (-)	3	2.25	1.5
Tank height, H_i (m)	3	2.81	2.25
Tank volume, V_{tank} (m ³)	2.36	3.45	3.98
Tank fill ratio, ff (-)	0.85	0.85	0.85
Volume of mix, V_{mix} (m ³)	2	2.93	3.38
Residence time, t_r (h)	1.7	2.35	2.64
Crystal growth rate, G (m/s)	7.24×10^{-8}	5.59×10^{-8}	5.09×10^{-8}
Mean crystals size, L_m (mm)	1.63	1.74	1.78

Table 4
EZ and FC design data

Parameter	Units	Electrolyzer data		Fuel cell data	
		Common data [41,45]	This project design	Common data [41,44]	This project design
Current density (i)	kAmps/m ²	2~10	4.67	1~10	4
Electrode area ($A_{effective}$)	m ²	0.9~2.7	1	0.001~2 (nominal)	1
Current (I) per stack	kAmps	2~30	4.2	Up to 20	3.6
Cell voltage (E_{cell})	Volts	1.75~4	2.75	Up to 0.8	0.68
Efficiency ξ_{H_2}	%	80~96	85	Up to 65	55
$N_{cells}/Stack$	-	Up to 181	181	Up to 283	198
N -stacks	-	Up to 181	4	Up to 283	2
Hydrogen capacity	tons/d	Up to 148×103 (produced)	2.54	NA (consumed)	2.54
Temperature	°C	50~95	50~55	<120	<100
Electric rating	DC kWh/kg H ₂	Up to 91.44	86.11	Up to 11.77	9.97
Consumed by EZ					
Produced by FC					

into protons and electrons thanks to a specially embedded catalyst; a selective membrane allows only protons to go through to the cathodic side while forcing the electrons to follow an external conducting circuit to the cathode. This external flow of electrons is the electric power that could be drawn from this mechanism of hydrogen splitting which can then be used to power external systems or units.

Electric power may be drawn because a stream of oxygen O₂ (pure or in the air) from the cathode side reacts with hydrogen protons (H⁺) and circulating electrons (e⁻) to produce water. The reaction at the cathode is exothermic thus generating heat that can be utilized outside of the fuel cell. The electric power generated by a fuel cell is dependent on many factors, such as (i) the type of fuel cell, (ii) its size, (iii) the operating temperature, and (iv) the pressure at which gases are introduced. At best, a single fuel cell generates about 1 V which is not enough for any applications. Thus, a significant number of individual fuel cells should be combined in series to form a stack to produce enough electric power for a specific need. This “scalability” makes fuel cells ideal for a wide variety of applications, from

small-scale appliances (50–100 W) to homes (1–5 kW), and vehicles (50–125 kW).

All fuel cells have basically the same configuration: an electrolyte and two electrodes. Nonetheless, different types of fuel cells are available and are classified primarily by the nature of electrolytes used. In fact, it is the type of electrolyte which determines the kind of chemical reactions that take place in the fuel cell, the operating temperature range, and other factors that determine its most suitable applications [42,43].

2.6.1. Electrochemistry of a fuel cell

The two main reactions occurring in a PEM fuel cell are:



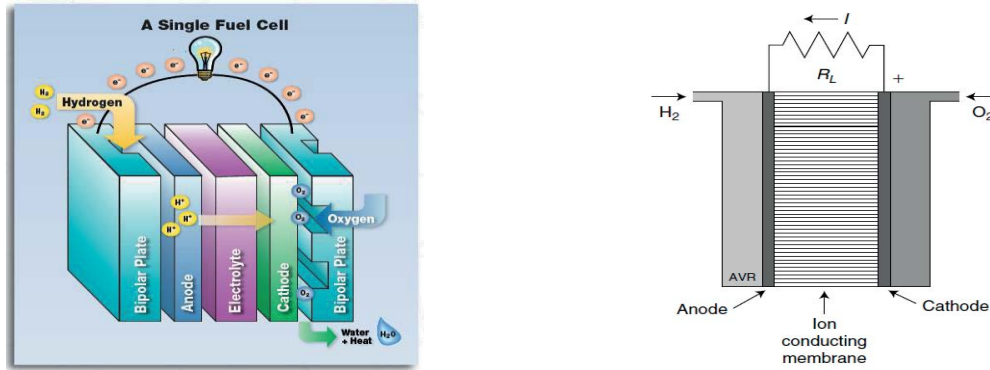


Fig. 8. Schematic of the fuel cell.

Similar to electrolyzer analysis [Eqs. (28)–(31)], the daily hydrogen molar consumption rate for 1 cell is:

$$\begin{aligned} \dot{m}_{H_2}^{(1\text{cell})} &= \tilde{Q}_{1\text{cell}} (\text{Amps} \cdot \text{s}) \times \frac{1(\text{mol} \cdot e^-)}{F(\text{C})} \times \frac{1(\text{mol} \cdot H_2)}{2(\text{mol} \cdot e^-)} \\ &= \frac{86,400 \times I}{2 \times F} \left(\text{mol} \cdot \frac{H_2}{d} \text{ per cell} \right) \end{aligned}$$

For an ideal fuel cell (efficiency $\xi_{H_2} = 100\%$), the number of cells will then be computed by:

$$N_{\text{cell,FC}} = \frac{\dot{m}_{H_2}^{(\text{total})}}{\dot{m}_{H_2}^{(1\text{cell})}} (\text{cells}) \quad (36)$$

$$\tilde{Q}_{\text{total}} = N_{\text{cell,FC}} \times \tilde{Q}_{1\text{cell}} = N_{\text{cell,FC}} \times I \times 86,400 (\text{in C/cell}) \quad (37)$$

The total power produced from the fuel cell is as follows:

$$P_{w,\text{FC}} = \eta_{\text{FC}} \times N_{\text{cell,FC}} \times I_{\text{cell,FC}} \times V_{\text{cell,FC}} \quad (38)$$

Table 4 summarizes pertinent operating values for fuel cell usage and the present design assumed values.

3. Results and discussion

The process equations are solved using the operating conditions given in Tables 1 and 2 for the basic structure, that is, S1. The numerical results are listed in Table 5 for mass flow rate and Table 6 for the composition. The resulted Key Performance Indicators (KPI) for this configuration is listed in Table 7. With the aid of the proposed method, the water recovery increased from 40% to 60%, and consequently, the liquid rejection is reduced from 60% to 40%. However, this achievement is obtained at a large energy requirement of 694 kW and a specific energy requirement of 941 kWh/m³. However, the ZLD process is known for its high cost due to its huge energy consumption [15]. Lu et al. [7] reported specific energy requirements that range between 2,000–2,700 kWh/m³. Schwantes et al. [15] suggested that a new strategy or technology be developed to make ZLD more economical. This is not the main focus here. Instead, the feasibility of generating renewable energy within the system is

investigated. The contribution of the different processing units to the required energy is shown in Fig. 9. It is obvious that EZ dominates the other processes in terms of energy requirements. In fact, EZ consumes 3,356 kW which corresponds to 98% of the total energy consumption. Indeed, EZ is known for its high specific energy requirement. For example, the specific energy requirement in terms of H₂ production ranges from 4.2 to 5.9 kWh/Nm³ H₂ for Alkaline Water Electrolysis (AWE) [39] and is theoretically about 3.6 kWh/Nm³ H₂ (or 40 kWh/kg H₂) for water splitting electrolysis. Although quite considerable energy is produced by the fuel cell (2,715 kW), it can barely offset that needed by the electrolyzer. The ED required energy is 38 kW which is equivalent to 16 kWh/m³ of ED feed. This value is slightly higher than the range of 7–15 kWh/m³ reported by Panagopoulos and Haralambous [13].

For a fair comparison of the 8 proposed configurations for the ZLD process, they were simulated using the nominal operating conditions. The KPI for these scenarios is shown in Fig. 10. The best scenario would be the one having the highest water recovery ratio and salt production and minimum rejection ratio and specific energy consumption. The notable observation is the behavior of S1c. This scenario owns the best waste liquid discharge of zero which meets the essence of the ZLD concept. In addition, it has the maximum solid salt production over all the scenarios. However, it suffers from very high energy consumption as well as high specific energy requirements. The reason for the considerable amount of energy consumption is related to the adverse effect of recycling streams as will be discussed further later. Thus, S1c is considered inferior to the rest of the configurations. Another observation is the superiority of the S2 configuration and its variants with respect to the S1 configuration and its variants. For example, the S2's deliver much higher water recovery and somehow smaller liquid rejection ratio with almost comparable salt production. However, the S2's consume more energy almost as twice that of the S1's. However, if we consider the specific energy requirement, the S2's become slightly less demanding. The definition of the specific energy demand played important role in differentiating the different scenarios. If the specific energy was defined as the ratio of the energy to the seawater feed, then the trend of GP_{ws} will be exactly similar to that of GP_w . In this sense, it loses its effect as a KPI to compare and distinguish the performance of

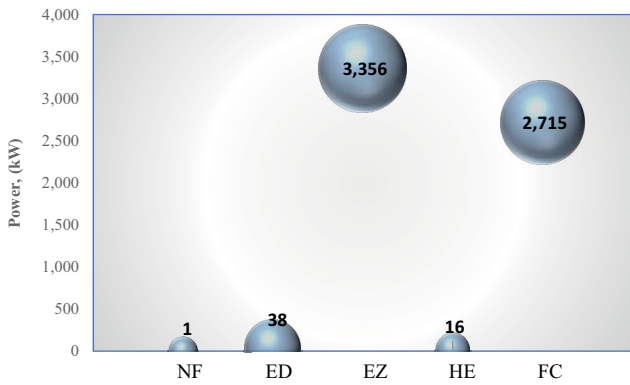


Fig. 9. Power requirement by different processes for S1 configuration.

the different scenarios. It was crucial to define the specific energy as the ratio of the required energy to the amount of pure water production because the proposed scenarios differ in their capability to increase water recovery and salt production. The S3 structure delivered an almost comparable performance with respect to the S2 configurations. However, S2b outperforms S3 in terms of higher salt production. Not to forget that the use of RO as a concentrator is questionable. Overall, S2b owns the best performance among the various structures.

To understand the effect of recycling on plant behavior, we break down the KPI shown in Fig. 10 for each configuration. Fig. 11 depicts the KPI exclusively for S1 and its variants. Excluding S1c, the figure indicated improvement in water recovery and consequently in salt production as they are related. Also, remarkable improvement in the liquid discharge percentage. The latter is intuitive because recycling will eliminate the liquid discharge. The aforementioned enhancement is obtained at small changes in the required energy and because of the increased water production, the specific energy demand is leveled off. Hence, it can be argued that recycling enhanced the performance at an additional minor cost. However, recycling harms the performance of the individual units which is overshadowed, except for S1c, by inspecting the overall energy requirement. To analyze this effect, we examine the results in Tables 8–10. Table 8 shows that the power demand of EZ dominates the other units which hide their corresponding changing power demand due to recycling. The power demand of EZ increases proportionally with RR because more energy is needed to convert the increased water inlet into hydrogen and oxygen. Nevertheless, Table 8 shows how the required transmembrane pressure and subsequently the pumping power for NF varies with the type of recycling. For S1 and S1c, the corresponding pressure and power change to 76,80 bar and 32,2263 kW, respectively. For S1b, the pressure and power do not change because stream 6 is recycled to the ED unit instead of the NF unit. These variations can be explained by inspecting the mass and composition balance listed in Table 9. Considering the S1a structure, the initial concentration of the recycle stream denoted by R0 in the table is 13,443 ppm which will dilute the NF feed after mixing with stream 3. Since

Table 5

Mass flow rate for all streams of S1 configuration (kg/d)

	1	2	3	4	5	6	7	8	9	10	11	12	13	14	15
H ₂ O	95,630	40,000	55,630	4,642	50,988	33,154	17,835	134	29,937	12,237				17,701	
Cl ⁻	2,409		2,409	482	1,927	289	1,638								
Na ⁺	1,340		1,340	268	1,072	161	911								
SO ₄ ⁻	338.40		338.40	331.63	6.77	1.02	5.75								
Mg ⁺⁺	161.80		161.80	158.56	3.24	0.49	2.75								
Ca ⁺⁺	50.80		50.80	49.78	1.02	0.15	0.86								
K ⁺	48.30		48.30	47.33	0.97	0.14	0.82								
HCO ₃ ⁻	13.00		13.00	12.74	0.26	0.04	0.22								
Br ⁻	8.30		8.30	8.13	0.17	0.02	0.14								
Si ⁺	0.01		0.01	0.01	0.00	0.00	0.00								
H ₂											1,967				1,967
O ₂												15,734	3,933	3,933	
N ₂													14,797	14,797	
NaOH															
NaCl (solid)								2,549							
Total	100,000	40,000	60,000	6,000	54,000	33,605	20,395	2,683	33,619	15,918	1,967	15,734	18,731	36,431	1,967

Table 6
Component concentration in the main streams, ppm

Species	1	2	3	4	5	6	7
H ₂ O	956,304	1,000,000	927,173	773,667	944,229	986,557	874,483
Cl ⁻	24,090		40,150	80,300	35,689	8,602	80,321
Na ⁺	13,400		22,333	44,667	19,852	4,785	44,679
SO ₄ ⁻	3,384		5,640	55,272	125	30	282
Mg ⁺⁺	1,618		2,697	26,427	60	14	135
Ca ⁺⁺	508		847	8,297	19	5	42
K ⁺	483		805	7,889	18	4	40
HCO ₃ ⁻	130		217	2,123	5	1	11
Br ⁻	83		138	1,356	3	1	7
Si ⁺	0.1		0.2	1.5	0.0	0.0	0.0
• ions	43,696		72,827	226,333	55,771	13,443	125,517

Table 7
KPI of S1 configuration

Parameter	Value
RR (%)	60
Rej. (%)	40
Salt (kg/d)	2,683
GP _w (kW)	694
GP _{ws} (kWh/m ³)	941

the NF has a high recovery ratio of 0.9 and mainly rejects non-NaCl ions, a large amount of water will be pushed into stream 5. Hence, the composition of stream 5 will be diluted further causing problems for the ED unit. Since the extraction level is fixed to depletion rate (DR) = 0.85 and the concentration level to Csc = 0.125, the ED will divert the augmented incoming water towards the dilute stream (the recycle stream). Hence, the recycle stream is amplified and recycled back to the NF. At a steady state, the recycle stream will approach a large value of 304,961 kg/d, which is almost ten times the original value. This amplified circulation rate will cause a minor effect on the energy requirement of the ED because its power requirement depends mainly on the extraction extent. The propagated inlet flow rate will affect the number of required ED cells which will influence the total power but marginally. On the other hand, the propagated circulation rate will amplify the NF energy requirement considerably. First, the required transmembrane pressure of NF will increase to maintain the desired recovery ratio of enlarged inlet flow rate. Note the osmotic pressure has less effect in this case because the feed concentration is diluted. As a result, the power demand of NF will amplify because it is directly proportional to both the feed pressure and the feed volumetric flow rate. The situation intensifies for S1c. The initial recycle mass rate is higher than that of S1a and the concentration is not as dilute as before. However, the recycle stream is more populated with TDS other than NaCl which is largely rejected in the NF unit. As a result, a larger amount of diluted solution is produced by the FN and sent to the ED. As mentioned

Table 8
Required power for S1 configuration and its variants

Parameter	S1	S1a	S1b	S1c
P _{NF} (bar)	21	76	21	80
P _{w,NF} (kW)	1	32	1	2,263
P _{w,ED} (kW)	38	69	77	106
P _{w,EZ} (kW)	3,356	3,813	3,948	4,820

earlier, the ED will produce a more dilute stream because DR and Csc are fixed. Note the concentration level, in this case, will reach up to 145,000 ppm because DR targets the total TDS rather than the NaCl ions and the ED feed solution contains traces of other TDS due to premixing with stream 4. Eventually, the recycle stream mass rate accumulates to a very large magnitude which is almost six hundred times the original flow rate. In due course, the power demand of NF soars to an extent it approaches 50% of that of the EZ unit and thus affects the overall energy demand as shown in Fig. 11 for the S1c system.

A similar situation occurs for the S1b configuration as shown in Table 10. It is not judicial to recycle a rejected stream by the ED to its own feed. Obviously, the recycle stream soared almost 900 times the original mass rate. Fortunately, the amplified circulation rate did not amplify the power demand considerably for the same reasons mentioned earlier. Regardless of the impact of waste recycling on the energy demand, it has a detrimental effect on unit performance. The expanded circulation rate may become beyond the designed capacity of the processing unit. Moreover, it may accelerate fouling and/or corrosion.

Fig. 12 illustrates the breakdown of the KPI for the S2 configuration and its generations. Once again, waste recycling enhances the overall performance. Increased water recovery ratio, increased salt production, and reduced waste rejection ratio are observed. The power demand is increased, but the specific power demand is leveled off due to the variable water production. Minor differences in GP_w and GP_{ws} are observed but it is not shown due to numerical rounding. Therefore, the ZLD plant with S2b configuration

Table 9
Mass flow rate and composition for selected stream of S1, S1a and S1c

System	Unit	3	3 + 6	4	5	6	7	R0
S1	kg/d	60,000	60,000	6,000	54,000	33,605	20,395	–
	ppm	72,827	72,827	226,333	55,771	13,443	125,517	–
S1a	kg/d	60,000	364,596	36,460	328,136	304,961	23,176	33,605
	ppm	72,827	13,392	40,101	10,424	1,682	125,457	13,443
S1c	kg/d	60,000	24,050,506	2,405,051	21,645,455	21,615,463	29,992	39,605
	ppm	72,827	1,747	15,334	237	36	145,692	45,694

Table 10
Mass flow rate and composition for selected streams of S1 and S1b

System	Unit	5	5 + 6	6	7	R0
S1	kg/d	54,000	54,000	33,605	20,395	–
	ppm	55,771	55,771	13,443	125,517	–
S1b	kg/d	54,000	30,004,621	29,980,628	23,994	33,605
	ppm	55,771	118	18	125,517	13,443

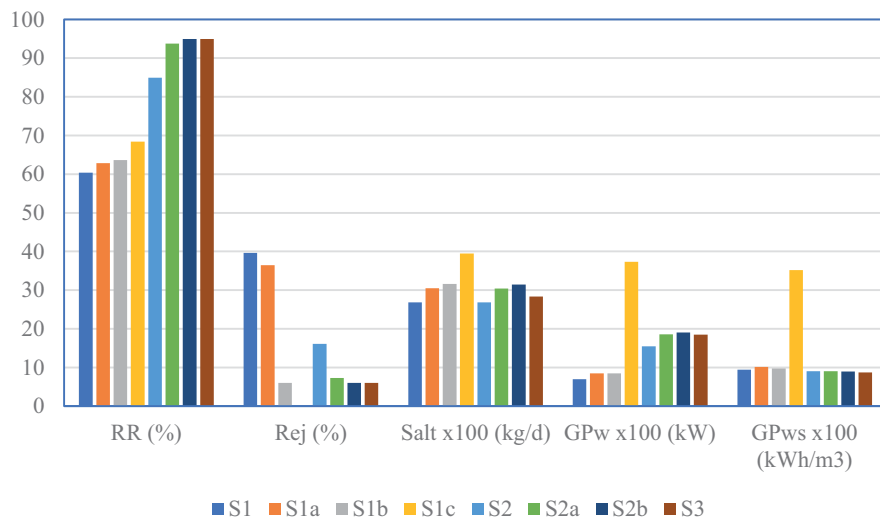


Fig. 10. KPI for the different configurations.

can achieve a waste liquid discharge as low as 6% and an overall water recovery of 95%, which is 55% beyond the desalination plant, at a specific energy of 900 kWh/m³. Unlike S1 with recycle, the waste recycling to join the NF feed (S2a) or the ED feed (S2b) does not create an augmented recycle mass rate. In due course, the initial mass rate of the recycle (stream 16) is small almost one-third of the recycle stream in S1 (stream 6). Moreover, the initial salinity of stream 16 is quite high around 43,000 ppm. Accordingly, the recycle stream does not dilute the feed of the NF or the ED. Nevertheless, recycling in the S2 structure can still incur operational limitations, especially in the ED unit as will be discussed in the following sections.

As mentioned earlier, the S3 configuration delivered comparable performance to that of S2b. However, besides

being idealistic, the RO operated at the maximum recovery ratio and allowable feed pressure. Thereby, further optimization of the RO operation is not possible. However, the ED unit parameters can be adjusted for better performance. For example, the ED can be used to concentrate the salt beyond 125,000 ppm by increasing the Csc parameter or produce further diluted products by increasing DR. In the following we examine the effect of DR and Csc on the ED performance and subsequently on the overall plant. In general, increasing DR will increase the amount of concentrate stream and consequently the amount of water associated with it. Increasing Csc will increase the salt portion in the concentrate stream and thus reduces the water associated with it.

The result is shown in Fig. 13 for the S1 configuration. Fig. 13a displays the effect of DR and Csc on the overall water

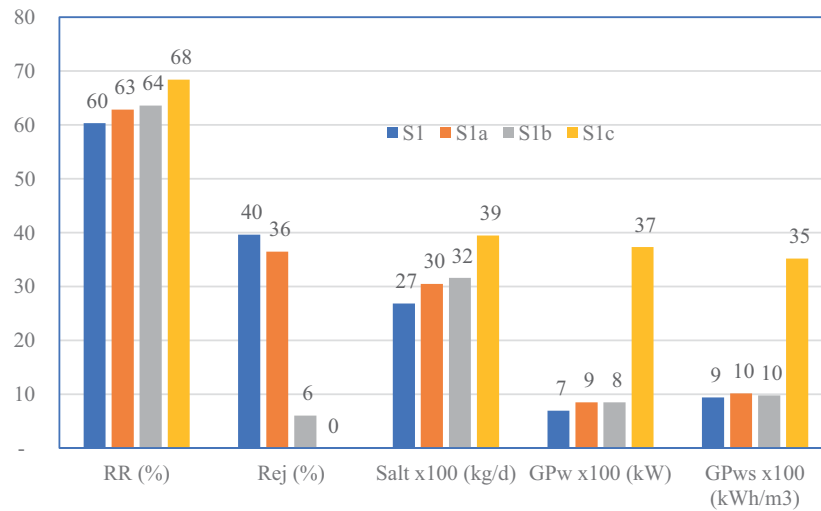


Fig. 11. KPI for the S1 configuration and variants.

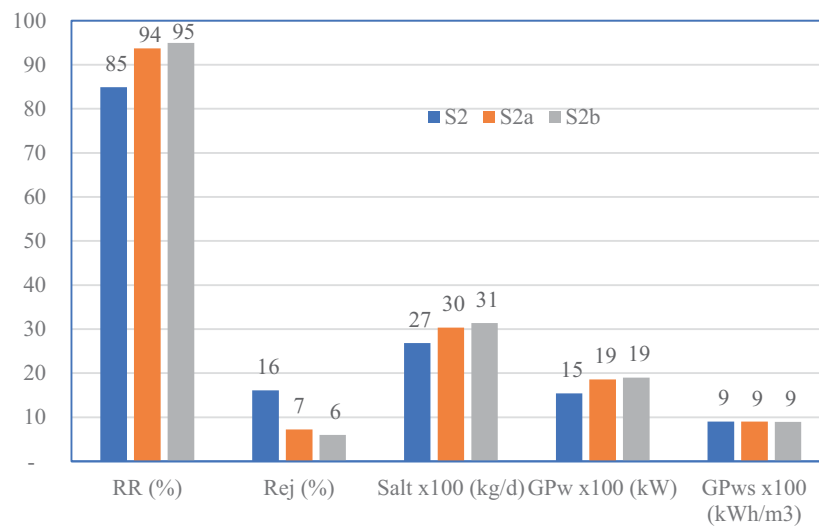


Fig. 12. KPI for the S2 configuration and variants.

recovery. Basically, increasing DR and reducing C_{sc} will increase the amount of water associated with a concentrated stream. At very low DR, the salt concentration (C_{sc}) has little effect but a considerable impact at higher values for DR. Similarly, at a very low value of C_{sc} , DR has a minor influence on the overall water recovery. Nevertheless, the maximum water recovery is obtained at the highest DR of 0.9 and the lowest C_{sc} of 0.075. In this case, the overall water recovery approaches about 78%. However, the maximum achievable recovery is still less than that of the S3 and S2 generations. Of course, the energy requirement will increase with an increase in water recovery because the EZ unit will consume more energy to convert the increasing amount of produced water. It should be reminded that EZ energy demand dominates the total energy requirements. In this case, the trend of the total energy demand will be similar to the water recovery demand. In contrast, the specific energy demand will demonstrate the opposite trend as shown in Fig. 13b. In this

case, the specific energy is lowest at the lowest C_{sc} for all values of DR. The highest specific energy occurs at the highest C_{sc} but increases with DR where it exceeds 1,150 kWh/m³ at DR = 0.9 and C_{sc} = 0.325. Therefore, it is recommended to operate at the lowest C_{sc} to guarantee the highest water recovery and minimum specific energy demand.

Fig. 14 illustrates the effect of DR and C_{sc} on the performance of S2 configuration to study the influence of adding RO to treat the ED effluent. Fig. 14a shows the water recovery trend which is similar to that for S1 with the highest recovery can reach up to 90%. Hence, high water recovery can be achieved by incorporating RO instead of recycling the waste stream like in S1a, b, c structures. However, the highest achievable water recovery is still lower than that of S2b. Unlike the case of S1, the water recovery trend for S2 at very high C_{sc} values, for example, 0.325 and 0.275, remains constant for all values of DR. In fact, the trend for C_{sc} = 0.325 drops marginally at DR = 0.9.

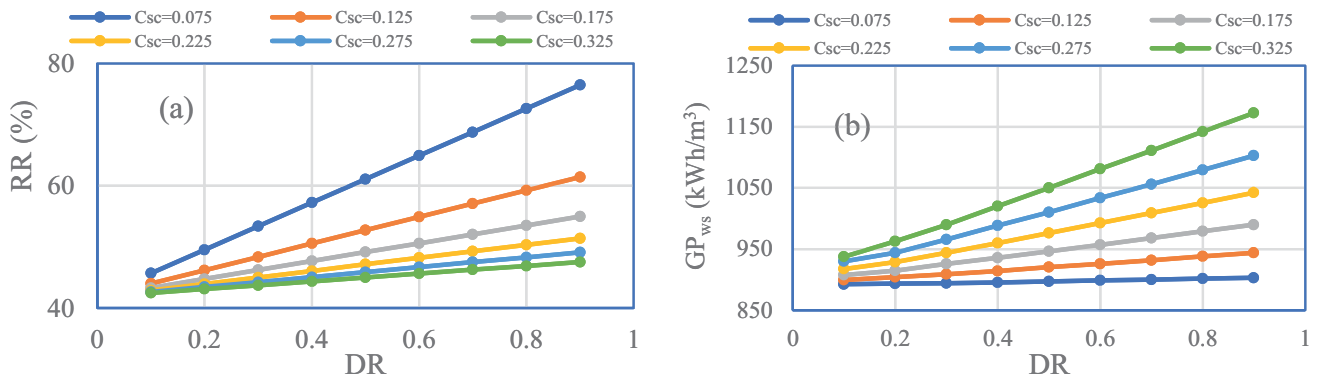


Fig. 13. Effect of ED design parameter on overall water recovery ratio and power density for S1 configuration.

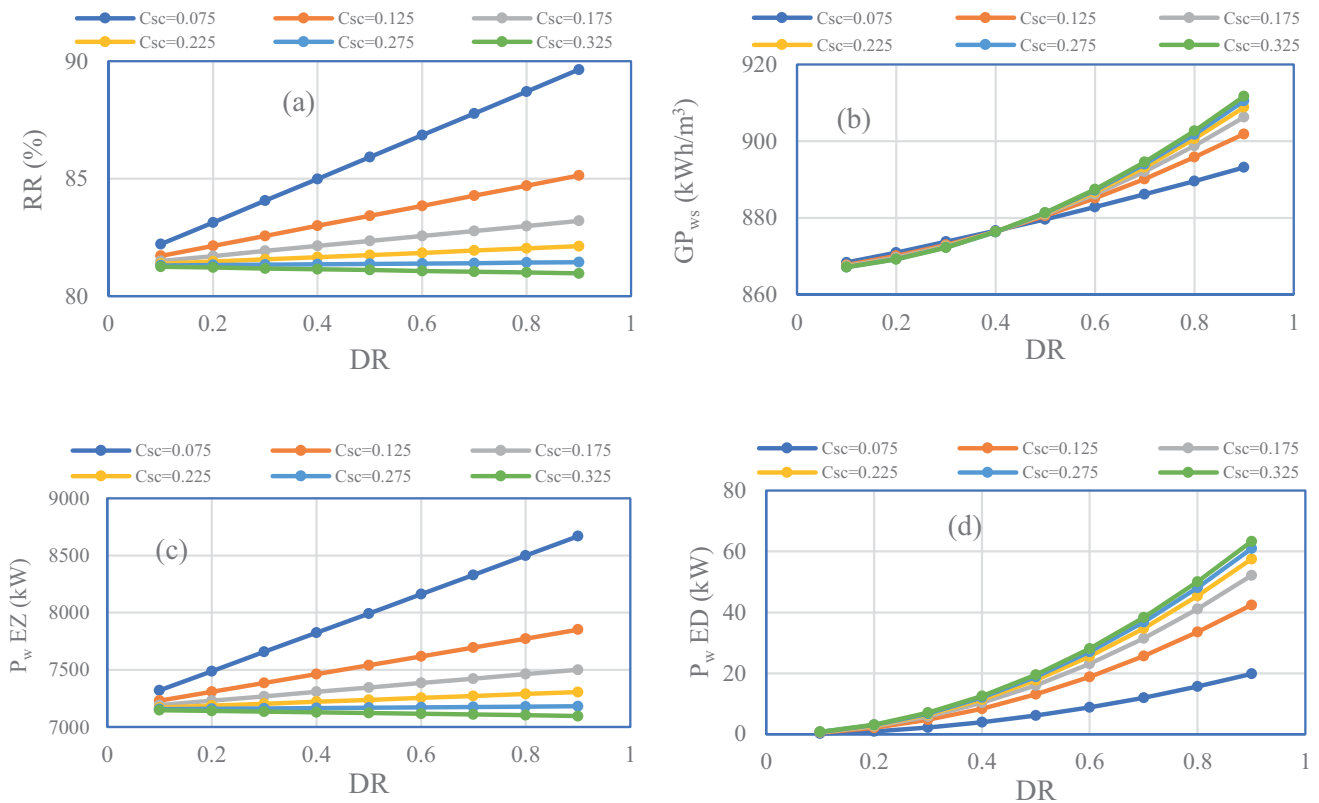


Fig. 14. Effect of ED design parameters on overall performance for S2 configuration.

For S2, the water recovery is the sum of that obtained from the ED and the following RO this is why S2 produces more water than S1. When DR increases for any value of Csc, the water produced by ED will increase. Hence, for a fixed RO recovery ratio, the water produced from RO will decrease proportionally. Since the amount produced by ED dominates at low Csc values, the total produced water will have the same trend as the ED concentrate with respect to DR and Csc. At high Csc, water produced from ED slightly increases with DR, hence, balanced by the water recovered by RO, the total produced water becomes asymptotic. Fig. 14b depicts the variation of the ED power demand which indicates propagation with both DR and

Csc but linearly at low Csc and exponentially at high Csc values. This is common because the power demand of ED depends on the degree of salt separation. Thus, $P_{w,ED}$ grows with extraction level (DR) and concentrating level (Csc). The energy demand of the EZ is proportional to the extent of water recovery as demonstrated in Fig. 14c. This is intuitive because the energy of EZ is directly proportional to the amount of water to be converted into hydrogen. The trend of the specific energy for S2 is shown in Fig. 14d which displays different behavior than that for S1 shown in Fig. 13b. The growth rate in GP_{ws} remains almost the same for all values of Csc up to DR = 0.5. This is because the trend of both RR and GP_w either has the same rate or

stays constant in that period. For DR values higher than 0.5, the extent of concentrating starts influencing the specific power as the latter grows rapidly with Csc.

Fig. 15 demonstrates the impact of the ED design parameter on the overall performance for the S2b configuration, that is, when the RO brine is recycled to the ED feed solution. As shown in Fig. 15a, the overall water recovery remains constant for all values of Csc and DR except for very minor changes with respect to DR. Although the water production from ED will still vary with design parameters, but the overall water production will remain constant because it is balanced with RO production with zero discharge. Due to the recycling of stream 16, the total water produced must be equal to that of the NF effluent (stream 5 before mixing). In due course, recycling eliminates the role of the ED design parameters, thus optimizing the ED operation does not affect the overall water recovery. Nevertheless, recycling affects the ED operation which is obscured in Fig. 15a because the lines are overlapping. This limitation is apparent in the other parts of Fig. 15. For example, Fig. 15b, shows the power density as a function of DR and Csc. Like S1 and S2, GP_{ws} increase with DR and Csc. However, at low DR and Csc values, the ED dumps more TDS into the dilute stream (S6) which is concentrated further in the RO and recycled to the ED feed. Consequently, the ED feed becomes highly concentrated to the extent it exceeds the target concentration set by Csc value. Therefore, the ED does not function properly or operates reversely, that is, becomes a diluter instead of a concentrator. For instance, at Csc = 0.075, the ED can only operate in the DR range of 0.7–0.9. The range increases with Csc value. However,

the minimum allowable DR is 0.2 even for the highest value of Csc. Fig. 15c illustrates the power demand of EZ which is constant because it is directly proportional to the amount of water recovered shown in Fig. 15a. Although, RR and P_w of EZ, which dominates the total power demand, are constant over all values of DR and Csc, the specific energy (GP_{ws}) depicted variation with these parameters. This is ascribed to the contribution of the energy demand of the other units especially the RO and ED as shown in Fig. 15d. Although the magnitude of the ED and RO power is minor relative to that of EZ, it contributes to the total power demand because the power of EZ is constant over the range of ED parameters. Not to forget that the power of EZ is reduced by subtracting the sizeable FC power and further scaled down by dividing by the recovered water.

Here we summarize the effect of recycling on the performance of S1 and S2 configurations. In S1, recycling the dilute S6 will deteriorate the performance of ED. Since the ED feed becomes diluted, it becomes difficult to maintain the concentration target of 125,000 ppm (i.e., fixed Csc at 0.125). Hence the only way to achieve the desired concentration is by pushing more water to the dilute stream which will amplify the recycle stream. Note the slightly improved overall recovery in S1a, S1b, and S1c is mainly due to the inflated ED feed rate. However, this is not the case for S2 because the recycle stream (S16) is not diluted as its salinity reaches 43,000 ppm. Moreover, the mass rate of S16 is small relative to the ED feed mass rate.

It is of benefit to operate ED at the highest concentration level (say 0.325) because it will improve the crystallization performance. It is common to concentrate the solution

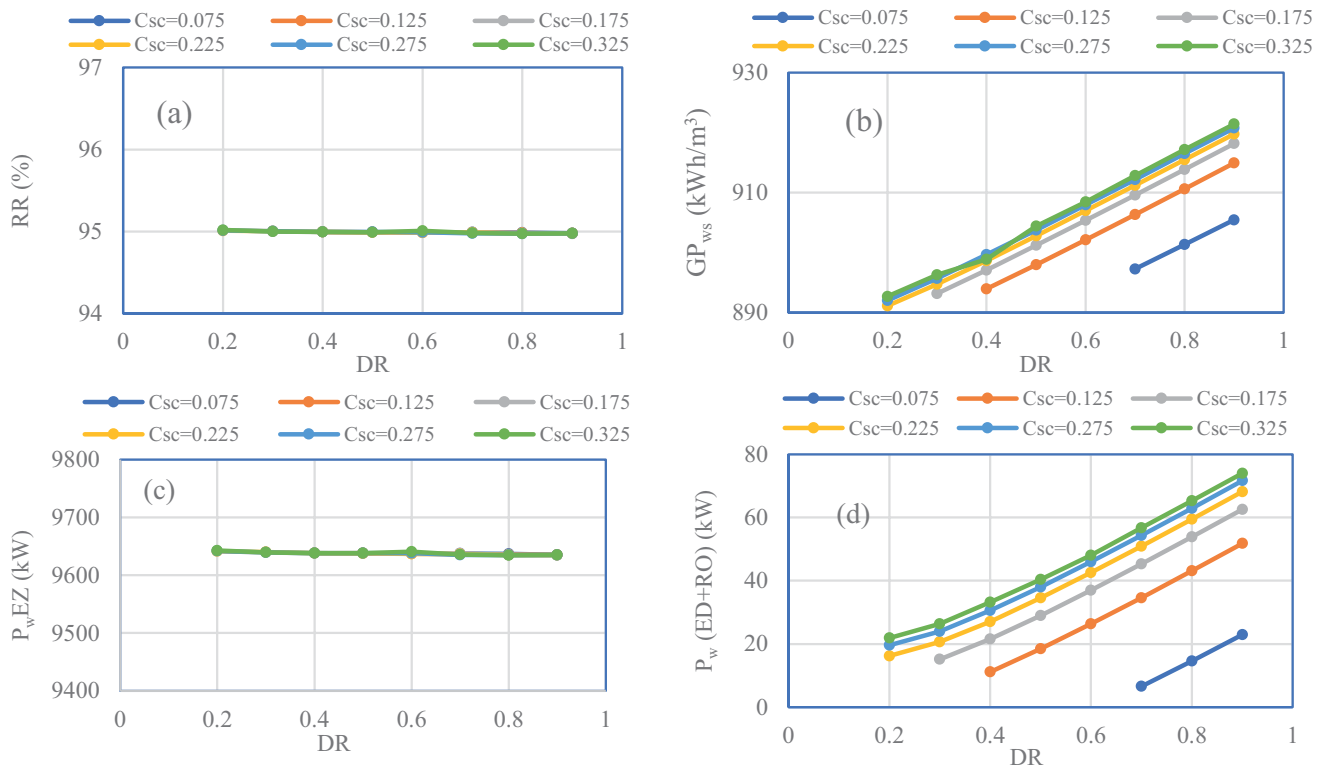


Fig. 15. Effect of ED design parameters on overall performance for S2b configuration.

to the saturation limit to reduce the energy required for crystallization [25]. However, for S1 this situation is associated with a low water recovery of around 47%. With the aid of RO (S2 configuration), the water recovery at the highest Csc can be improved to around 81%. Furthermore, recycling the RO brine (S2b configuration) helped even to increase the overall recovery to almost 95%. Hence, the use of RO and recycling can help operate ED at the highest concentration level without sacrificing water recovery.

Due to the promising performance of the S2 configuration, we further study the impact of increasing the recovery ratio of the RO unit on the overall performance. Note, that the RO feed has a small mass flow rate and low concentration of 12,000–15,000 ppm. Thereby there is room to increase the recovery ratio which will of course increase the required transmembrane pressure and subsequently the power demand. Fig. 16 depicts the effect of the RO recovery ratio on plant performance. Fig. 16a displays the resulted KPI for the S2 structure where the RO brine is discharged to the environment. Obviously, increasing the recovery ratio from 0.7 to 0.9 managed to improve the water recovery from 85% to 92% and consequently reduces the liquid discharge from 16% to 9%. However, the amount of produced salt remains constant because it is governed by the concentration level in the ED. Not shown in the figure, the RO power increases from 1.0 to 1.8 kW and the EZ power from 7,812 to 9,082 kW. However, the growth in water production flattened the specific energy to around 900 kWh/m³. Two significant digits were displayed in Fig. 16a for GP_{ws} to signify its minor variation. Fig. 16b shows the influence of RO recovery ratio on S2b configuration where the RO brine is recycled to the ED feed. In due course, increasing the RO recovery ratio from 0.7 to 0.9 does not affect the water recovery because it is already reached the maximum allowable value via recycling. The liquid discharge is also unaffected because the RO brine is simply recycled instead of discharged to the environment. The salt production is marginally altered because of the effect of the salt in the recycle stream on the separation mechanism inside the ED unit. Similarly, the specific energy demand is unaltered because EZ power demand is unchanged. It is true, that the RO power demand increases from 1 to 2 kW, which is not shown here, but its contribution is concealed by the ample power demand of the EZ unit.

Nevertheless, when the RO brine is recycled, increasing the RO recovery cannot help improve the overall performance.

4. Conclusions

In this work, a process to treat the desalination waste for zero liquid discharge is proposed. The proposed plant uses an electro dialysis for salt concentration. In addition, an electrolyzer followed by a fuel cell is incorporated to produce green energy as a side product. Different configurations involving waste recycling, adding additional RO units to treat the liquid waste, and replacing the electro dialysis with a typical RO for salt concentrating are studied. The various configurations are compared to concentrate 7.3% brine solution up to 12.5%. It is found that the energy demand is high where the specific energy can reach 900–1,000 kWh/m³ of total produced pure water. 98% of the energy demand is incurred by the electrolyzer. Although considerable energy can be produced by the fuel cell, but it can suffice only 80% of the energy consumed by the electrolyzer. The energy efficiency of the plant can be improved if supported by free renewable energy such as solar and/or wind energies. Recycling the liquid waste directly to the same processing unit can provide a slight improvement in the overall performance. However, it can harm the process operation such as causing an inflated recirculation rate and, in some cases, dramatic growth in the energy demand. Hence, achieving full nil liquid discharge may not be without cost. On the other hand, further treatment of the water liquid by an RO in this study can enhance the overall plant performance to achieve 95% pure overall water recovery, 6% waste liquid discharge, and 3,142 kg/d of solid salt production at a specific energy demand of 900 kWh/m³. It is also found that recycling the waste liquid after processing by RO in this study, can help enhance the overall performance but may limit the range of operability of the subsequent unit, that is, the ED in this case.

Acknowledgment

This project is funded by the Researchers Supporting Project number (RSP2022R510), King Saud University, Riyadh, Saudi Arabia.

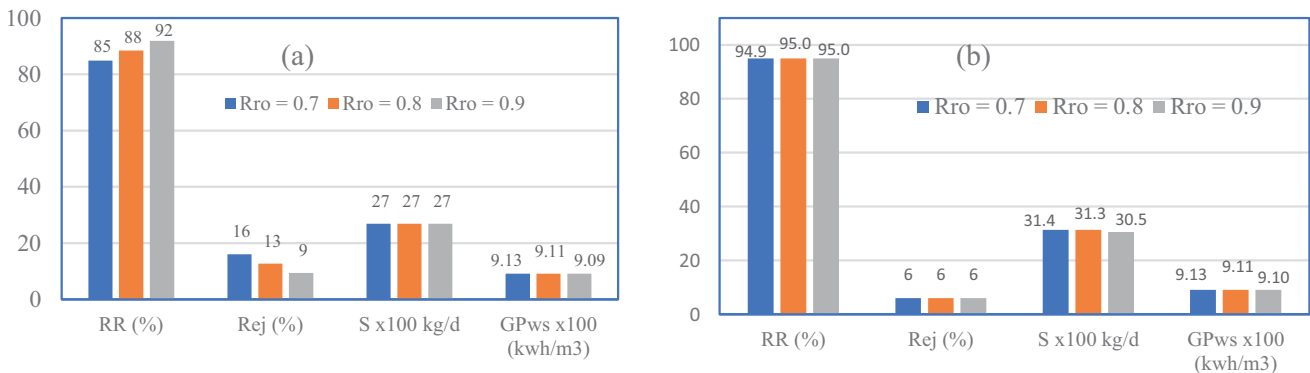


Fig. 16. Effect of recovery ratio of the supporting RO unit; (a) S2 and (b) S2b.

Symbols

A	—	RO membrane permeability, m/d/bar
C	—	Concentration, ppm
\dot{C}	—	Salt ionic concentration, keq/m ³
D	—	Tank diameter, m
DR	—	Degree of desalination
F	—	Faraday constant (96,485.44 C/keq)
ff	—	Fill fraction
G	—	Crystal growth rate, m/s
GP_w	—	Gross power demand, kW
GP_{ws}	—	Specific gross power, kWh/m ³
H	—	Tank height, m
I	—	Total passing current through a cell pair, Amps
J_w	—	Solvent flux, m/d
K	—	Constant for polarization factor
k_R, k_V	—	Empirical constants for the crystalizer
L_m	—	Crystal mean size, m
m_i	—	Mass rate of stream i , kg/d
m	—	Mass rate, kg/d
N	—	Number of cell-pairs
r_{pore}	—	Pore radius, m
R	—	Recovery ratio
RR	—	Overall recovery of water
Rej	—	Waste liquid reaction ratio
R_j	—	Reject ratio
P_w	—	Power, kW
PF	—	Polarization factor
Q	—	Volumetric flow rate, m ³ /s
\tilde{Q}	—	Cell charge, Amps
Q^d, Q^c	—	Flow rates of dilute and concentrate solutions in the cells parallel to the membrane surface (m ³ /s)
S	—	Solid salt production, kg/d
S_A	—	Membrane surface area, m ²
t_r	—	Residence time, s
TRP	—	Total required power, kW
TGP	—	Total generated power, kW
z	—	Anion/cation charge number (i.e., $z = 1$ for Na ⁺ , Cl ⁻)

Greek

ρ	—	Density, kg/m ³
η	—	Efficiency
π	—	Osmotic pressure, Pa
μ	—	Solvent viscosity, kg/m·s
ξ	—	Current efficiency
\dot{v}	—	Magma flow rate, m ³ /s

Subscripts/superscripts

b	—	Brine
c	—	Concentrate
Cell	—	Fuel cell
d	—	Dilute
el	—	Electrical
f	—	Feed
p	—	Permeate
s	—	Salt
ED	—	Electrodialysis

EZ	—	Electrolyzer
FC	—	Fuel cell
NF	—	Nanofiltration
RO	—	Reverse osmosis

References

- [1] UNESCO, The United Nations World Water Development Report 2020: Water and Climate Change, United Nations Educational, Scientific and Cultural Organization, 2020.
- [2] C. Charcosset, A review of membrane processes and renewable energies for desalination, *Desalination*, 245 (2009) 214–231.
- [3] N. Ghaffour, T.M. Missimer, G.L. Amy, Technical review and evaluation of the economics of water desalination: current and future challenges for better water supply sustainability, *Desalination*, 309 (2013) 197–207.
- [4] J. Eke, A. Yusuf, A. Giwa, A. Sodiq, The global status of desalination: an assessment of current desalination technologies, plants and capacity, *Desalination*, 495 (2020) 114633, doi: 10.1016/j.desal.2020.114633.
- [5] V.G. Gude, Desalination and sustainability—an appraisal and current perspective, *Water Res.*, 89 (2016) 87–106.
- [6] Z. Zhang, O.R. Lokare, A.V. Gusa, R.D. Vidic, Pretreatment of brackish water reverse osmosis (BWRO) concentrate to enhance water recovery in inland desalination plants by direct contact membrane distillation (DCMD), *Desalination*, 508 (2021) 115050, doi: 10.1016/j.desal.2021.115050.
- [7] K.J. Lu, Z.L. Cheng, J. Chang, L. Luo, T.-S. Chung, Design of zero liquid discharge desalination (ZLDD) systems consisting of freeze desalination, membrane distillation, and crystallization powered by green energies, *Desalination*, 458 (2019) 66–75.
- [8] A.J. Toth, Modelling and optimisation of multi-stage flash distillation and reverse osmosis for desalination of saline process wastewater sources, *Membranes*, 10 (2020) 265, doi: 10.3390/membrane10100265.
- [9] M. Cappelle, W.S. Walker, T.A. Davis, Improving desalination recovery using zero discharge desalination (ZDD): a process model for evaluating technical feasibility, *Ind. Eng. Chem. Res.*, 56 (2017) 10448–10460.
- [10] A. Panagopoulos, K.-J. Haralambous, M. Loizidou, Desalination brine disposal methods and treatment technologies - a review, *Sci. Total Environ.*, 693 (2019) 133545, doi: 10.1016/j.scitotenv.2019.07.351.
- [11] I.S. Al-Mutaz, Msf challenges and survivals, *Desal. Water Treat.*, 177 (2020) 14–22.
- [12] I.S. Al-Mutaz, Features of multi-effect evaporation desalination plants, *Desal. Water Treat.*, 54 (2015) 3227–3235.
- [13] A. Panagopoulos, K.-J. Haralambous, Minimal liquid discharge (MLD) and zero liquid discharge (ZLD) strategies for wastewater management and resource recovery – analysis, challenges and prospects, *J. Environ. Chem. Eng.*, 8 (2020) 104418, doi: 10.1016/j.jece.2020.104418.
- [14] M. Ahmed, D. Hoey, W.H. Shayya, M.F. Goosen, Brine disposal from inland desalination plants: current status, problems, and opportunities, In: Volume II of Environmental Sciences and Environmental Computing (Electronic Book Series), EnviroComp Consulting, Inc., CA 94539, USA.
- [15] R. Schwantes, K. Chavan, D. Winter, C. Felsmann, J. Pfafferoth, Techno-economic comparison of membrane distillation and MVC in a zero liquid discharge application, *Desalination*, 428 (2018) 50–68.
- [16] G.P. Thiel, E.W. Tow, L.D. Banchik, H.W. Chung, Energy consumption in desalinating produced water from shale oil and gas extraction, *Desalination*, 366 (2015) 94–112.
- [17] R.L. McGinnis, N.T. Hancock, M.S. Nowosielski-Slepowron, G.D. McGurgan, Pilot demonstration of the NH₃/CO₂ forward osmosis desalination process on high salinity brines, *Desalination*, 312 (2013) 67–74.
- [18] R. Creusen, J. van Medevoort, M. Roelands, A. van Renesse van Duivenbode, J.H. Hanemaaijer, R. van Leerdam, Integrated membrane distillation–crystallization: process design and cost

- estimations for seawater treatment and fluxes of single salt solutions, *Desalination*, 323 (2013) 8–16.
- [19] G. Guan, R. Wang, F. Wicaksana, X. Yang, A.G. Fane, Analysis of membrane distillation crystallization system for high salinity brine treatment with zero discharge using Aspen flowsheet simulation, *Ind. Eng. Chem. Res.*, 51 (2012) 13405–13413.
- [20] F. Edwie, T.-S. Chung, Development of simultaneous membrane distillation–crystallization (SMDC) technology for treatment of saturated brine, *Chem. Eng. Sci.*, 98 (2013) 160–172.
- [21] E.K. Summers, H.A. Arafat, Energy efficiency comparison of single-stage membrane distillation (MD) desalination cycles in different configurations, *Desalination*, 290 (2012) 54–66.
- [22] F. Tahir, S.G. Al-Ghamdi, Integrated MED and HDH desalination systems for an energy-efficient zero liquid discharge (ZLD) system, *Energy Rep.*, 8 (2022) 29–34.
- [23] D.U. Lawal, M.A. Antar, A.E. Khalifa, Integration of a MSF desalination system with a HDH system for brine recovery, *Sustainability*, 13 (2021) 3506, doi: 10.3390/su13063506.
- [24] K. Loganathan, P. Chelme-Ayala, M.G. El-Din, Treatment of basal water using a hybrid electrodialysis reversal–reverse osmosis system combined with a low-temperature crystallizer for near-zero liquid discharge, *Desalination*, 363 (2015) 92–98.
- [25] T.A. Davis, Zero Discharge Seawater Desalination: Integrating the Production of Freshwater, Salt, Magnesium, and Bromine, Desalination and Water Purification Research Development Program Report No. 111, University of South Carolina, USA, 2007.
- [26] J. Chang, J. Zuo, K.-J. Lu, T.-S. Chung, Membrane development and energy analysis of freeze desalination–vacuum membrane distillation hybrid systems powered by LNG regasification and solar energy, *Desalination*, 449 (2019) 16–25.
- [27] S. Kumarasamy, S. Narasimhan, S. Narasimhan, Optimal operation of battery-less solar powered reverse osmosis plant for desalination, *Desalination*, 375 (2015) 89–99.
- [28] D.W. Solutions, Filmtec™ Reverse Osmosis Membranes, Technical Manual, Form 399, 2010, pp. 1–180. Available at: <https://www.rainmandesal.com/wp-content/uploads/2018/09/dow-filmtec-sw30-manual.pdf>, (Accessed 10-8-2022).
- [29] M. Khayet, Membranes and theoretical modeling of membrane distillation: a review, *Adv. Colloid Interface Sci.*, 164 (2011) 56–88.
- [30] S. Lin, N.Y. Yip, M. Elimelech, Direct contact membrane distillation with heat recovery: thermodynamic insights from module scale modeling, *J. Membr. Sci.*, 453 (2014) 498–515.
- [31] A. Ghorbani, B. Bayati, E. Drioli, F. Macedonio, T. Kikhavani, M. Frappa, Modeling of nanofiltration process using DSPM-DE model for purification of amine solution, *Membranes*, 11 (2021) 230, doi: 10.3390/membranes11040230.
- [32] Y. Roy, M.H. Sharqawy, Modeling of flat-sheet and spiral-wound nanofiltration configurations and its application in seawater nanofiltration, *J. Membr. Sci.*, 493 (2015) 360–372.
- [33] S. Adham, T. Gilgoly, E. Hansen, G. Lehman, E. Rosenblum, Comparison of Advanced Treatment Methods for Partial Desalting of Tertiary Effluents, US Department of the Interior, Bureau of Reclamation, 2009. Available at: <https://www.usbr.gov/research/dwpr/reportpdfs/report097.pdf>, (Accessed 10-8-2022).
- [34] D. Andriollo, Experimental and Modeling-based Evaluation of Electrodialysis for the Desalination of Watery Streams, Master Thesis, University of Padoua, Padoua, Italy, 2014.
- [35] W. Juda, W.A. McRae, Coherent ion-exchange gels and membranes, *J. Am. Chem. Soc.*, 72 (1950) 1044–1044.
- [36] H. Strathmann, Ion-Exchange Membrane Separation Processes, Elsevier, Amsterdam, The Netherlands, 2004.
- [37] S. Misztal, D. Verdoes, Investigation Into Methods to Increase the Crystal Size in Suspension Melt Crystallization of Caprolactam, Proceedings of the 14th Symposium on Industrial Crystallization, Cambridge, UK, 1999.
- [38] A. Bamberger, R. Eek, A. Fellholter, H.-P. Wirges, Investigation of a Cooling Crystallization of an Organic Compound by Combining Laboratory Experiments, Simulation and Plant Experiments, Proceedings of the 14th International Symposium on Industrial Crystallization (CD-ROM), Cambridge, UK, 1999.
- [39] G. Amikam, P. Nativ, Y. Gendel, Chlorine-free alkaline seawater electrolysis for hydrogen production, *Int. J. Hydrogen Energy*, 43 (2018) 6504–6514.
- [40] U. DOE, DOE Technical Targets for Hydrogen Production from Electrolysis, 2018. Available at: <https://www.energy.gov/eere/fuelcells/doe-technical-targets-hydrogen-production-photoelectrochemical-water-splitting>, (Accessed 10-8-2022)
- [41] K.W. Harrison, R. Remick, A. Hoskin, G. Martin, Hydrogen Production: Fundamentals and Case Study Summaries, National Renewable Energy Lab (NREL), Golden, Co., United States, 2010.
- [42] F. Barbir, PEM electrolysis for production of hydrogen from renewable energy sources, *Sol. Energy*, 78 (2005) 661–669.
- [43] B.T. Scheffler, S. Heidrich, Fixing the Specification of the ‘To-Be-Developed’ Stacks, Stack Components and Manufacturing Systems, European Commission Report Fit-4-AMandA D1.1, 2017. Available at: <https://ec.europa.eu/research/participants/documents/downloadPublic?documentIds=080166e5b4b51faa&appId=PPGMS>
- [44] S. Jancic, P.A. Grootcholten, Industrial Crystallization, Springer, Springer, USA, 1984.
- [45] Y. Kuang, M.J. Kenney, Y. Meng, W.-H. Hung, Y. Liu, J.E. Huang, R. Prasanna, P. Li, Y. Li, L. Wang, Solar-Driven, Highly Sustained Splitting of Seawater Into Hydrogen and Oxygen Fuels, Proceedings of the National Academy of Sciences, USA, 116 (2019) 6624–6629.